Indian J. Phys. **81** (5 & 6), 607-614 (2007)

IJP

Deep inelastic neutrino scattering and fractal models of nucleon structure functions at small x

D K Choudhury* and Rupjyoti Gogoi

Department of Physics, Gauhati University, Guwahati – 781 014, Assam, India

E-mail dkc_phys@yahoo.co in

Received 5 October 2006, accepted 16 May 2007

Abstract : The concept of self-similarity in the structure of the proton at small x used successfully in the analysis of recent HERA data, is now extended to deep inelastic neutrino scattering. The fractal models are then tested with the available CCFR neutrino data

Keywords · Self-similarity, fractal dimension, deep inelastic scattering, structure function, low x

PACS Nos. . 05.45.Df, 12 38.-t, 13 60.Hb

1. Introduction

While notion of self-similarity and fractals has been extensively studied in hadron multiparticle production processes during last decades [1-7], its application in deep inelastic scattering is rather more recent when Lastovicka [8,9] proposed a functional form of the structure function $F_2(x,Q^2)$ reflecting self-similarity at small x and could provide an excellent description of HERA data [10,11] with the fitted parameters D_1, D_2 and D_3 identified as fractal or self-similar dimensions. Later [12], the monofractal limit of Lastovicka's model was studied in an analogy with classical monofractals [13,14] as well as with a variant of statistical quark model [15]. More recently [16], a new parameterization of proton structure function at small x has been proposed to overcome the problem of negativity of one of the fractal dimension D_3 of the proposed fractal model.

The present paper makes a similar analysis of the nucleon structure functions in deep inelastic neutrino scattering. Unfortunately, the deep inelastic neutrino scattering experiments

Corresponding Author

have not yet explored the very small x values unlike the corresponding electron-proton scattering experiments. The CCFR neutrino scattering data are available [17,18] in the kinematic range $0.0075 \leq x \leq 0.75$ and $1.3 \leq Q^2 \leq 125.9\ GeV^2$. This is to be compared with HERA data [10,11] which cover a region of four momentum transferred squared $0.045 \leq Q^2 \leq 150\ GeV^2$ and of Bjorken x, $6.2\text{x}10^{-7} \leq x \leq 0.2$. In spite of this kinematical constraint on DIS neutrino data, in the present paper, we will test the validity or otherwise of the fractal models pursued in electron-proton scattering and see if any new insight can be obtained from this rather novel approach of looking at the structure of the proton.

In Section 2, we develop the formalism while Section 3 is devoted to the results and discussions.

2. Formalism

As noted in Ref. [16], two alternative forms of the unintegrated parton densities $f_i(x,q^2)$ are available:

$$\log f_i\left(x,q^2\right) = D_1 \log 1/x \log\left(Q_0^2 + q^2/Q_0^2\right) + D_2 \log 1/x + D_3 \log\left(Q_0^2 + q^2/Q_0^2\right) + D_0' \quad (1)$$

and

$$\log f_i\left(x,q^2\right) = D_1 \log 1/x \log\left(Q_0^2/Q_0^2 + q^2\right) + D_2 \log 1/x + D_3 \log\left(Q_0^2/Q_0^2 + q^2\right) + D_0', \quad (2)$$

where D_1, D_2, D_3 are the flavor independent self-similarity dimension and D_0' are the flavor dependent normalization constants.

Integrating over q^2, one obtains the integrated parton densities $q_i(x,Q^2)$ as

$$q_i\left(x,Q^2\right) = \int_0^{Q^2} f_i\left(x,q^2\right) dq^2 . \quad (3)$$

The structure function F_2 and xF_3 are given as [19]:

$$F_2^{\nu N} = x\left(\bar{u}+\bar{d}\right) + x(d+u)\left[\,|V_{ud}|^2 + |V_{cd}|^2\,\right] + 2xs\left[\,|V_{us}|^2 + |V_{cs}|^2\,\right] + 2xs \quad (4)$$

and

$$xF_3^{\nu N} = -x\left(\bar{u}+\bar{d}\right) + x(d+u)\left[\,|V_{ud}|^2 + |V_{cd}|^2\,\right] + 2xs\left[\,|V_{us}|^2 + |V_{cs}|^2\,\right] - 2xs, \quad (5)$$

where $u=u(x,Q^2)$ *etc* and V_{if} are the CKM matrix elements [20].

Here, $$F_2^{\nu N} = \frac{F_2^{\nu p} + F_2^{\nu n}}{2} \tag{6}$$

and $$xF_3^{\nu N} = \frac{xF_3^{\nu p} + xF_3^{\nu n}}{2} \tag{7}$$

Using (1) and (2) in eqs. (4) and (5), we get two sets of structure functions.

Set I:

$$F_2^{\nu N}\left(x,Q^2\right) = \frac{e^{D_0'} Q_0^2 x^{-D_2+1}}{1+D_3+D_1\log 1/x} \times \left(x^{-D_1 \log\left(1+Q^2/Q_0^2\right)} \left(1+Q^2/Q_0^2\right)^{D_3+1} - 1 \right) \tag{8}$$

and $$xF_3^{\nu N}\left(x,Q^2\right) = \frac{e^{D_0''} Q_0^2 x^{-D_2+1}}{1+D_3+D_1\log 1/x} \times \left(x^{-D_1 \log\left(1+Q^2/Q_0^2\right)} \left(1+Q^2/Q_0^2\right)^{D_3+1} - 1 \right). \tag{9}$$

Set II:

$$F_2^{\nu N}\left(x,Q^2\right) = \frac{e^{D_0'} Q_0^2 x^{-D_2+1}}{1-D_3-D_1\log 1/x} \times \left(x^{D_1 \log\left(1+Q^2/Q_0^2\right)} \left(1+Q^2/Q_0^2\right)^{-D_3+1} - 1 \right) \tag{10}$$

and $$xF_3^{\nu N}\left(x,Q^2\right) = \frac{e^{D_0''} Q_0^2 x^{-D_2+1}}{1-D_3-D_1\log 1/x} \times \left(x^{D_1 \log\left(1+Q^2/Q_0^2\right)} \left(1+Q^2/Q_0^2\right)^{-D_3+1} - 1 \right), \tag{11}$$

where the normalization constants D_0' and D_0'' are appropriate combinations of flavor dependent constants D_0^i occurred in (1) and (2):

$$e^{D_0'} = \left[e^{D_0^{\bar{u}}} + e^{D_0^{\bar{d}}} \right] + \left[e^{D_0^{d}} + e^{D_0^{u}} \right] \left[|V_{ud}|^2 + |V_{cd}|^2 \right] + 2e^{D_0^{s}} \left[|V_{us}|^2 + |V_{cs}|^2 \right] + 2e^{D_0^{c}}, \tag{12}$$

$$e^{D_0''} = -\left[e^{D_0^{\bar{u}}} + e^{D_0^{\bar{d}}} \right] + \left[e^{D_0^{d}} + e^{D_0^{u}} \right] \left[|V_{ud}|^2 + |V_{cd}|^2 \right] + 2e^{D_0^{s}} \left[|V_{us}|^2 + |V_{cs}|^2 \right] - 2e^{D_0^{c}}. \tag{13}$$

3. Results and discussion

The numerical values of the self-similarity dimensions D_1, D_2 and D_3 as well as Q_0^2 are already determined from DIS HERA data and reported in Refs. [8] and [16]. The flavor dependent normalization constants D_0' and D_0'' are determined from CCFR data and are recorded in Tables 1, 2.

Table 1. Results of fit for $D_1=0$ and $D_1 \neq 0$ for $1.3 \leq Q^2 \leq 125\,9$ GeV^2 and $0.0075 \leq x \leq 0.35$ for Ref.[8] and Ref. [16].

	F_2						xF_3					
	D_1 fixed			D_1 fitted			D_1 fixed			D_1 fitted		
Fit	D_0'	χ^2	χ^2 /dof	D_0'	χ^2	χ^2 /dof	D_0''	χ^2	χ^2 /dof	D_0''	χ^2	χ^2 /dof
Ref.[8]	2.1205 ±0.263	12.143	0.136	1.9078 ±0.262	11.653	0.131	4.1574 ±0.698	217.766	2.447	4.3462 ±0.560	365 525	4 107
Ref.[16]	2.0803 ±0.220	4.159	0.047	2.2628 ±0.215	5.934	0.067	4.1057 ±0.456	78.452	0.881	4.1755 ±0.470	92.001	1.034

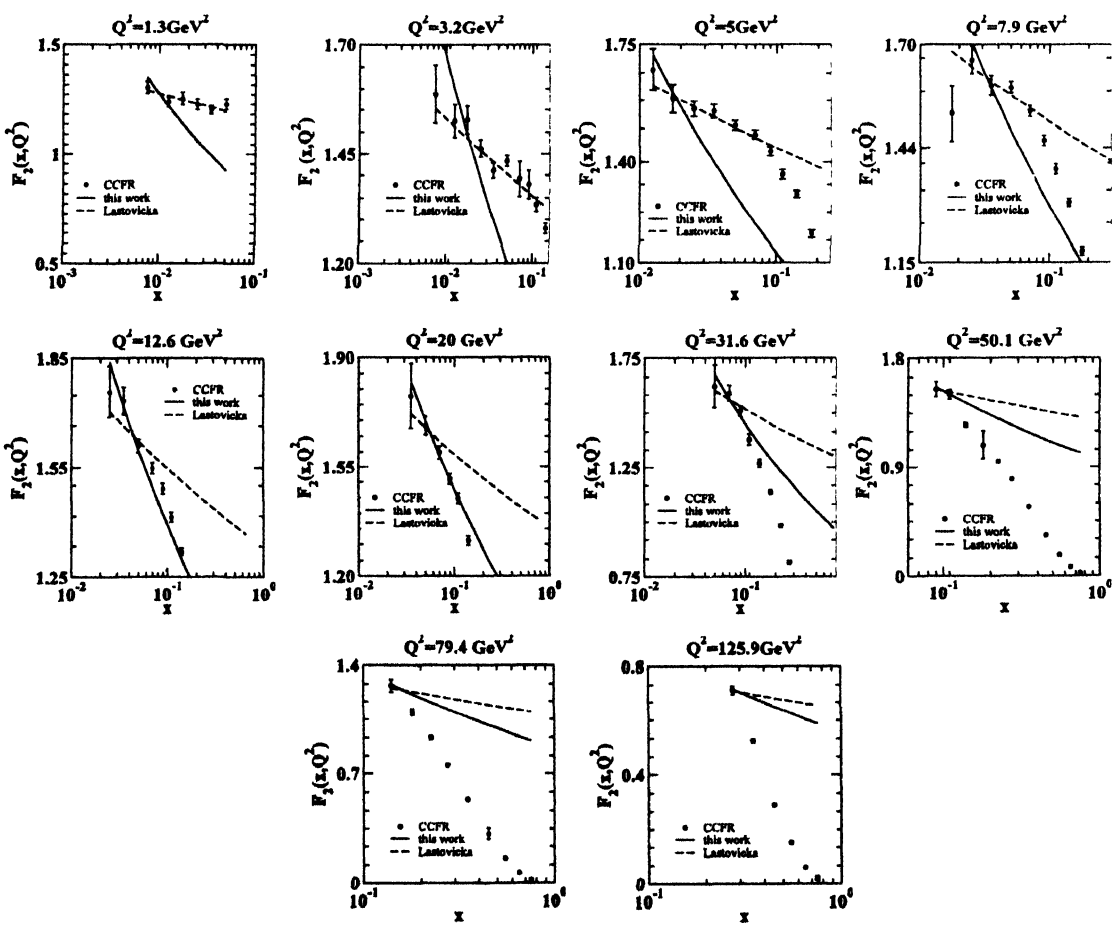

Figure 1. $F_2(x,Q^2)$ *versus* x in bins of Q^2 with $D_1 = 0$ (eqs. 8 &10).

Table 2. Results of the fit for $D_1=0$ and $D_1 \neq 0$ for $1\ 3 \leq Q^2 \leq 20$ GeV^2 and $0.0075 \leq x \leq 0.35$ for Ref. [8] and Ref. [16].

	F_2						xF_3					
	D_1 fixed			D_1 fitted			D_1 fixed			D_1 fitted		
Fit	D_0'	χ^2	χ^2 /dof	D_0'	χ^2	χ^2 /dof	D_0''	χ^2	χ^2 /dof	D_0''	χ^2	χ^2 /dof
Ref.[8]	2.1205 ±0.263	3.766	0.057	1.9078 ±0.262	3 456	0 052	4 1574 ±0.598	75.905	1.150 ±0 560	4 3462	130 864	1 983
Ref.[16]	2.0803 ±0.220	2.437	0 0369	2.2628 ±0.215	2 440	0 037	4.1057 ±0.456	29.095	0.441	4.1755 ±0.470	35.461	0.537

In Figures 1 and 2, we plot $F_2(x,Q^2)$ *vs* x in bins of Q^2 with $D_1 = 0$ and $D_1 \neq 0$, respectively. A study of Figure 1 for $F_2(x,Q^2)$ *vs* x (with $D_1 = 0$) shows that for lower values of Q^2 ($Q^2 < 5$ *GeV*^{2}), model of Ref. [8] fits better than that of Ref. [16]; but for intermediate Q^2 range (Q^2 = 12.6 - 20 *GeV*^{2}), the model of Ref. [16] is preferred by data. The predictions of both the models for each Q^2 bin are found to have a cross over point

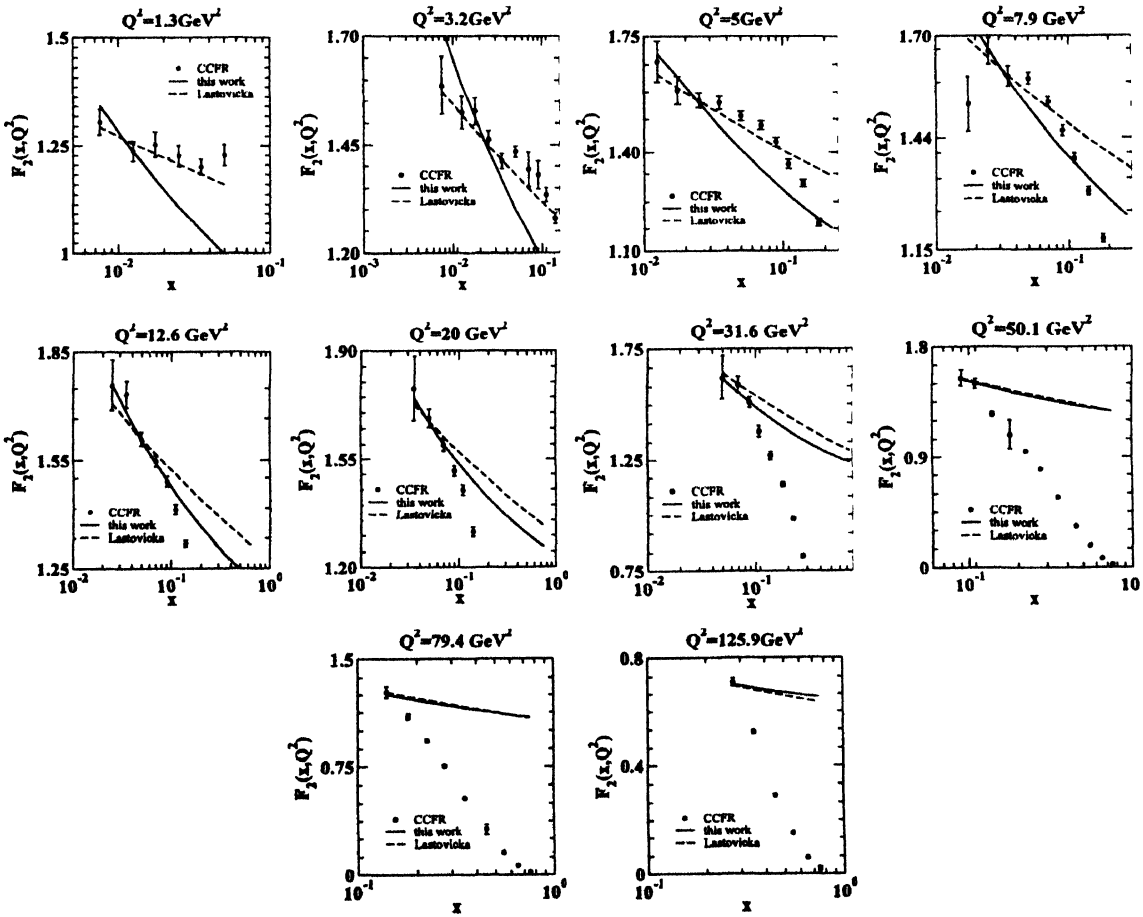

Figure 2. $F_2(x,Q^2)$ *versus* x in bins of Q^2 with $D_1 \neq 0$ (eqs. 8 &10).

at a particular point. As Q^2 is increased, the cross over point shifts towards large x. As an illustration while at $Q^2 = 1.3\ GeV^2$, the cross over point is at $x = 0.01$, at $Q^2 = 125.9\ GeV^2$, it shifts to $x = 0.298$. For higher Q^2 ($Q^2 > 20\ GeV^2$), however predictions of both the models overshot the data.

A similar pattern persists even for $F_2(x,Q^2)$ *vs* Q^2 with $D_1 \neq 0$ in Figure 2. The χ^2 for $1.3 \leq Q^2 \leq 125.9\ GeV^2$ and the lower Q^2 range $1.3 \leq Q^2 \leq 20\ GeV^2$ are shown in Table 1 and 2. From χ^2 analysis, the present model (Ref. [16]) fits better than that of Lastovicka (Ref. [8]). As expected, if confined to low Q^2 range ($Q^2 < 20\ GeV^2$), χ^2/dof is improved.

In Figures 3 and 4, we plot xF_3 *vs* x in bins of Q^2 with $D_1 = 0$ and $D_1 \neq 0$, respectively. Corresponding χ^2 are again shown in Tables 1 and 2, respectively. Except for low Q^2 range (which basically explores the smallest available x of CCFR data), both the models fail to reproduce the experimental pattern; rather they invariably overshot the data. This feature is presumably due to the predominant valence nature of non-singlet

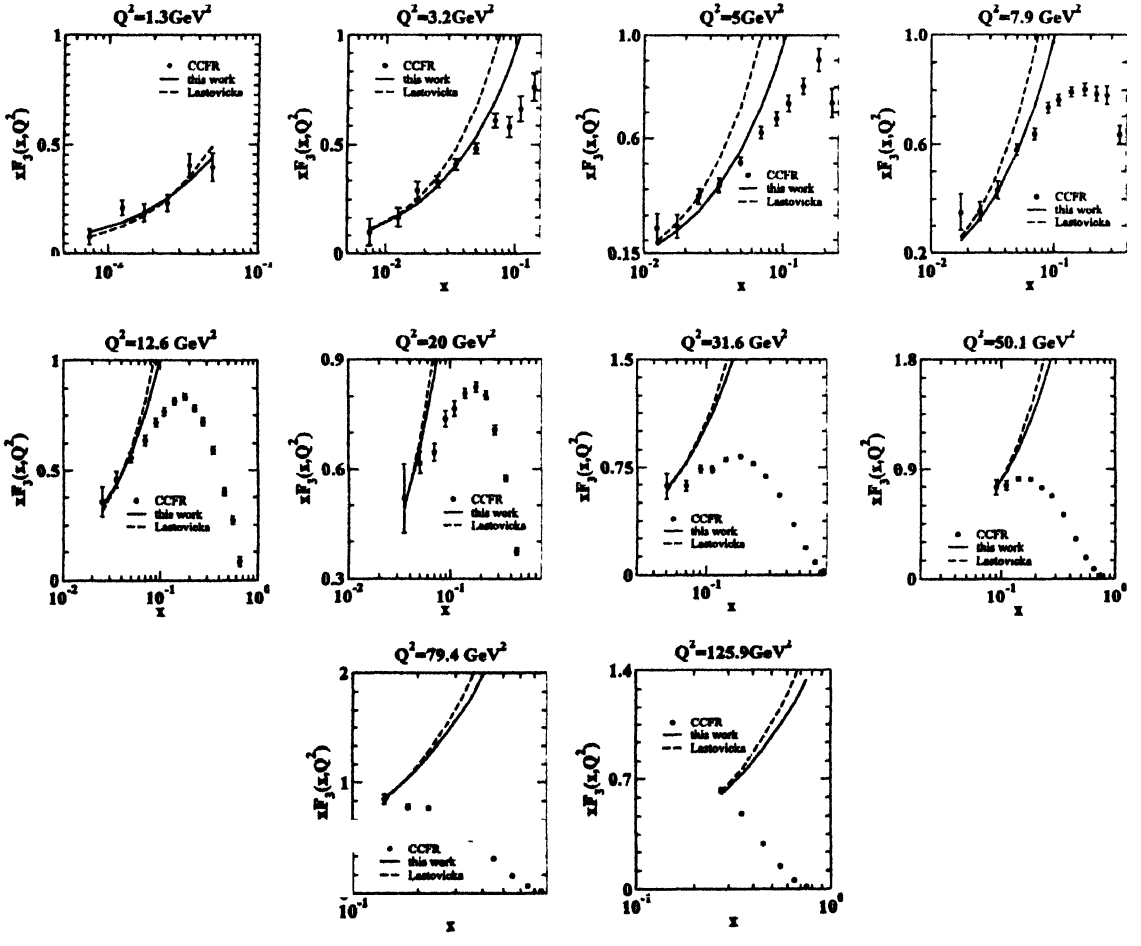

Figure 3. $xF_3(x,Q^2)$ *versus* x in bins of Q^2 with $D_1 = 0$ (eqs. 9 &11).

structure function $F_2(x,Q^2)$ where the probability of gluon radiation creating self-similar pattern is very small.

To conclude, while the fractal models of Refs. [8] and [16] provide an excellent description for the HERA data at small x, for CCFR neutrino data, the models have limited validity. This is most probably due to the fact that CCFR experiment has not yet reached the small x regime where the notion of self-similarity may be more appropriate. Future DIS neutrino experiment in such small x regime can alone provide fresh insight into the structure of the proton by interpreting the data based on fractality.

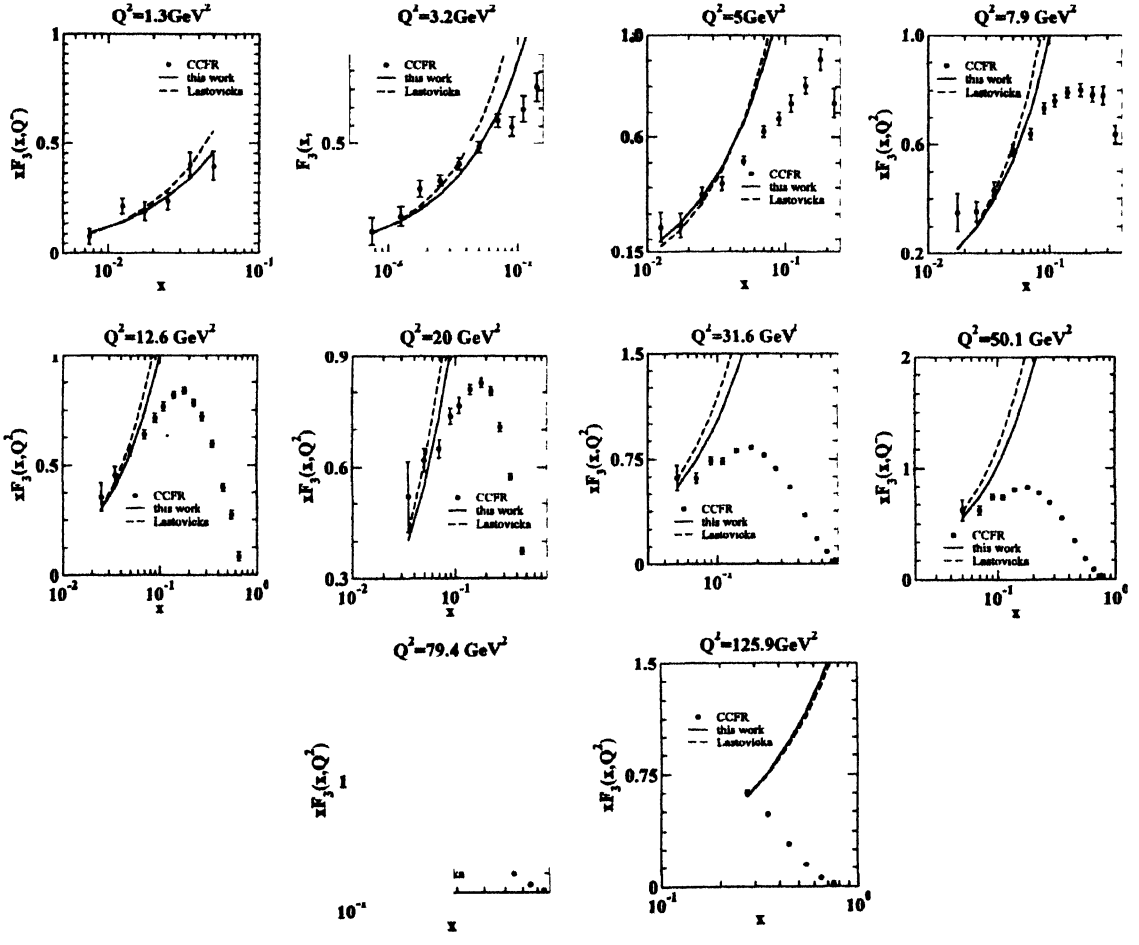

Figure 4. $xF_3(x,Q^2)$ *versus* x in bins of Q^2 with $D_1 \neq 0$ (eqs. 9 &11).

References

[1] I M Dremin *Mod. Phys. Lett.* **A3** 1333 (1988)

[2] R Lipa and B Buschbeck *Phys. Lett.* **B223** 465 (1989)

[3] R C Hwa *Phys. Rev.* **D41** 1456 (1990)

[4] W Florowski and R C Hwa *Phys. Rev.* **D43** 1548 (1991)

[5] W Yuanfung and L Lianshou *Int. J. Mod. Phys.* **A53** 37 (2003)

[6] D Ghosh, A Dev and S Pal *Indian J. Phys.* **79** 1395 (2005)

[7] D Ghosh *et al, Fractals* **13** 325 (2005)

[8] T Lastovicka *Euro. Phys. J.* **C24** 529 (2002); hep-ph/0203260

[9] T Lastovicka *Ph.D Thesis*, DESY-THESIS-2004-016, (Humboldt-University, Berlin) (2003)

[10] H1: C Adloff *et al, Euro. Phys. J.* **C22** 33 (2002); hep-ex/0012053

[11] ZEUS: J Brietweg *et al, Phys. Lett.* **B487** 53 (2000); hep-ex/0005018

[12] D K Choudhury and Rupjyoti Gogoi *Indian J. Phys.* **80** 659 (2006)

[13] BB Mandelbrot *Fractal Geometry of Nature* (New York: W H Freeman) (1983)

[14] Michael F Barnsley *Fractal Everywhere* (New York: Academic) (1993)

[15] S N Banerjee, A Bhattacharya, B Chakraborti and S Banerjee *Int. J. Mod. Phys.* **A17** 4939 (2002)

[16] D K Choudhury and Rupjyoti Gogoi *Indian J. Phys.* **80** 823 (2006)

[17] CCFR Collaboration: WC Leung *et al, Phys. Lett.* **B 317** 655 (1993)

[18] CCFR Collaboration: WJ Seligman *et al, Phys. Rev. Lett.* **79** 1213 (1997)

[19] M Ghick, S Kretzer and E Reya; astro-ph / 9809273

[20] Particle Data Group: C Caso *et al, Euro. Phys. J.* **C3** (1998)